Complex Complex Saddle-Node Bifurcations

Robert L. Devaney *

July 22, 2001

*Please address all correspondence to Robert L. Devaney, Department of Mathematics, Boston University, Boston MA 02215, or email bob@bu.edu.

1 Introduction

One of the simplest bifurcations in all of discrete or continuous dynamical systems theory is the *saddle-node bifurcation*. Roughly speaking, in this bifurcation, two fixed points (or periodic points) come together as a parameter is varied and then disappear.

Often, however, this purely local bifurcation is accompanied by extremely complicated global changes in the overall dynamics of the system. Nowhere is this more apparent than in complex dynamics, where the saddle-node bifurcation often leads to dramatic or "complex" changes in the structure of the Julia set.

In this paper, we will describe three examples of such bifurcations. The first occurs in the study of quadratic dynamical systems, specifically at the cusp of the main cardioid in the Mandelbrot set. This is the "simple" complex saddle-node bifurcation. The second occurs for more general polynomials, including the bifurcations that occur at the cusps of all other "baby" Mandelbrot sets. And the third occurs in the case of the complex exponential function, where a saddle-node bifurcation leads to an amazing explosion in the set of chaotic orbits. Incidentally, there is nothing special about the polynomial or exponential nature of the examples we consider: the first two examples can occur in families of rational maps, and the third occurs in a wide variety of entire functions.

Before discussing the complex versions of these bifurcations, recall the simple saddle-node bifurcation that occurs for maps of the interval. To be specific, consider the quadratic function $Q_c(x) = x^2 + c$. The fixed points for this map are given by

$$p_\pm = \frac{1}{2} \pm \frac{1}{2}\sqrt{1-4c}.$$

So there are no fixed points if $c > 1/4$; one fixed point when $c = 1/4$; and two fixed points when $c < 1/4$. This is the *saddle-node bifurcation*; at $c = 1/4$ a pair of fixed points suddenly appears as we lower the parameter c.

Now we have

$$Q_c'(p_\pm) = 1 \pm \sqrt{1-4c}.$$

Therefore $Q_c'(p_+) > 1$ for all $c < 1/4$ and $-1 < Q_c'(p_-) < 1$ for c in the interval $-3/4 < c < 1/4$. Hence p_+ is always a source while p_- is a sink for $-3/4 < c < 1/4$.

From a global point of view, this local saddle-node bifurcation is accompanied by a substantial change in the fate of orbits of the system. When

$c > 1/4$, all orbits tend to ∞. When $c = 1/4$ we have a single neutral fixed point at $x = 1/2$. The interval $(-1/2, 1/2)$ is the basin of attraction of this fixed point, and its left hand endpoint $x = -1/2$ is eventually fixed. All other orbits tend to ∞. For $-3/4 < c < 1/4$ a similar picture emerges. The interval $[-p_+, p_+]$ forms the set of bounded orbits, with interior points forming the basin of p_-. Outside this interval all orbits tend to ∞.

Thus we see that as c passes through $1/4$ there suddenly appears a "large" interval of bounded orbits, where for $c > 1/4$ there were no bounded orbits. This is the global bifurcation in this case. In the next section we will discuss the global ramifications of this bifurcation in the complex plane. Later we will turn to still more complicated complex saddle-node bifurcations.

This paper is dedicated to Prof. Floris Takens on the occasion of his sixtieth birthday. It is impossible for me to measure the profound effect Floris' work has had on my work and that of my students. It has been a pleasure over all of these years to learn from him and to share his excitement about dynamical systems.

2 The "Simple" Complex Saddle-Node

Now we turn to the complex version of the quadratic bifurcation described above, i.e., the bifurcation of the complex map $Q_c(z) = z^2 + c$ when c passes through $c = 1/4$. To keep matters simple, we will again assume that c is real. We will be most interested in the set of points whose orbits remain bounded. This set is called the *filled Julia set* of Q_c and is denoted by K_c. The boundary of this set is known as the *Julia set*. It is denoted by J_c. We are interested in the change in the geometry of these sets as c passes through the bifurcation point.

One of the fundamental facts from complex dynamics is the following:

Role of the critical orbit: Suppose P is a complex polynomial and assume that P has an attracting cycle. Then this cycle must attract at least one critical point of P.

In the case of $Q_c(z) = z^2 + c$, it follows that the orbit of 0 must tend to the attracting fixed point when $-3/4 < c < 1/4$. When $c > 1/4$, however, the orbit of 0 escapes to ∞. This has enormous consequences for the structure of the filled Julia set.

Before discussing this, we make a brief digression to describe the Fundamental Dichotomy of quadratic dynamics. The point at infinity is a superattracting fixed point for Q_c, i.e., it is a fixed point with derivative 0. By classical work predating Julia and Fatou, we may find a conjugacy near ∞ between Q_c and the squaring function $Q_0(z) = z^2$. That is, we may find a neighborhood U of ∞ and an analytic map

$$\phi_c : U \to \{z| \ |z| > r\}$$

for some $r > 1$ such that $\phi_c \circ Q_c = (\phi_c(z))^2$.

Now suppose that the orbit of 0 is bounded. In this case we can extend the conjugacy to $Q_c^{-1}(U)$ in the natural way. We get

$$\phi_c : Q_c^{-1}(U) \to \{z| \ |z| > \sqrt{r}\}$$

which again conjugates Q_c and Q_0. The impediment to this extension occurs if c belongs to U; in this case, c has only one preimage, namely 0, whereas any other $z \in U$ has two distinct preimages. This prevents us from extending ϕ_c to a well-defined function on $Q_c^{-1}(U)$.

So if c belongs to K_c, it follows that we can continue this process indefinitely. We thus extend ϕ_c to the entire basin of attraction of ∞ which we denote by W_c. Thus

$$\phi_c : W_c \to \{z| \ |z| > 1\}$$

gives a global conjugacy between Q_c and Q_0 on this basin.

The important observation here is that W_c is simply connected (each time we pull back a "disk" we obtain a "disk"). Therefore the complement of W_c is a closed, connected set. But the complement of W_c is just K_c.

Now if c lies in U, a very different topological picture emerges. To see this, suppose that c lies on the boundary of U. We can always arrange this by first modifying U and then pulling U back as above. What is $Q_c^{-1}(U)$? Well, each point in the boundary of U has two preimages with the exception of c, which has only one. So the preimage of the boundary of U is the figure eight curve shown in Figure 1, and the preimage of U is the exterior of this set.

So the complement of $\overline{Q_c^{-1}(U)}$ consists of two disks which we denote by D_0 and D_1. Q_c maps each of these disks in one-to-one fashion onto the disk which forms the complement of $\overline{U}$ (and contains both D_0 and D_1 in its interior). Therefore K_c is contained inside $D_0 \cup D_1$. We claim that this set has infinitely many connected components.

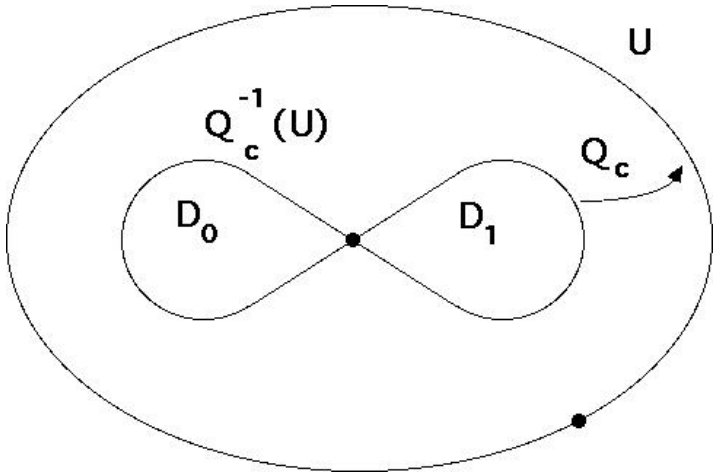

Figure 1: Pulling back via Q_c^{-1}.

To see this, let F_0 and F_1 denote the two branches of Q_c^{-1} defined on $D_0 \cup D_1$, with F_j taking values in D_j. Since $Q_c|D_j$ is one-to-one, both F_0 and F_1 are analytic. Now let $s = s_0 s_1 s_2 \ldots$ be an infinite sequence of 0's and 1's. We may form the infinite composition

$$F_{s_0 s_1 s_2 \ldots}(z) = \lim_{n \to \infty} F_{s_0} \circ F_{s_1} \circ \ldots \circ F_{s_n}(z)$$

for any z in $D_0 \cup D_1$. Note that this limit point must lie in K_c since $Q_c^n(F_{s_0 s_1 s_2 \ldots}(z))$ lies in $D_0 \cup D_1$ for each n. Furthermore, the itinerary of this limit point relative to D_0 and D_1 is given exactly by the sequence $s_0 s_1 s_2 \ldots$ that is,

$$F_{s_0 s_1 s_2 \ldots}(z) \in D_{s_0}$$

$$Q_c(F_{s_0 s_1 s_2 \ldots}(z)) = F_{s_1 s_2 \ldots}(z) \in D_{s_1}$$

and in general

$$Q_c^n(F_{s_0 s_1 s_2 \ldots}(z)) = F_{s_n s_{n+1}}(z) \in D_{s_n}.$$

As a consequence, if two sequences $s_0 s_1 s_2 \ldots$ and $t_0 t_1 t_2 \ldots$ disagree somewhere, say in the n^{th} spot, then the corresponding limit points lie in different components of K_c. (Q_c^n of one of these limit points lies in D_0; the other in D_1.) Thus the filled Julia set consists of uncountably many components.

Moreover, each component is a single point; that is $F_{s_0 s_1 s_2 \ldots}(z)$ is independent of z. This follows from the fact that both F_0 and F_1 are strict

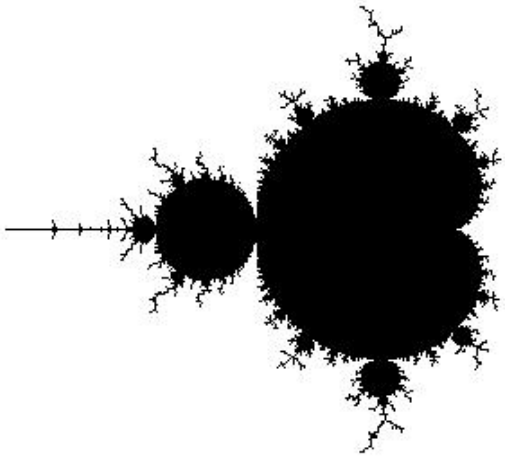

Figure 2: The Mandelbrot set.

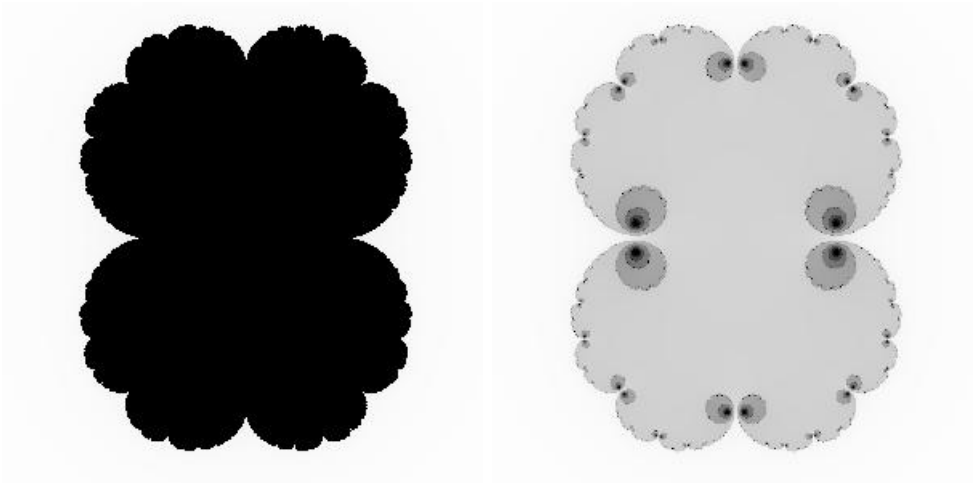

Figure 3: The Julia set when $c = 0.25$ and $c = 0.26$. The black points represent points in the filled Julia set; grey-scale points escape to ∞.

contractions on D_0 and D_1 in the Poincaré metric. So the distance between $F_{s_0} \circ \ldots \circ F_{s_n}(z_1)$ and $F_{s_0} \circ \ldots \circ F_{s_n}(z_2)$ decreases by a definite factor at each additional iteration. Consequently K_c is totally disconnected. It is also closed and perfect (this uses the fact that $F_{s_0 s_1 \ldots s_n o}(z)$ and $F_{s_0 s_1 \ldots s_n 1}(z)$ are close together). So we see that K_c is a Cantor set when $Q_c^n(0) \to \infty$.

This then gives us one of the major results in quadratic dynamics:

The Fundamental Dichotomy

1. *If $Q_c^n(0) \to \infty$, the filled Julia set of Q_c is a Cantor set.*
2. *If $Q_c^n(0) \not\to \infty$, the filled Julia set of Q_c is a connected set.*

Thus the filled Julia sets of quadratic functions come in one of only two forms: connected sets or totally disconnected sets. There are no quadratic filled Julia sets that consist of 2, 5, or 345,678 components.

Remark. As is well-known, the Mandelbrot set $\mathcal{M}$ is a picture of the Fundamental Dichotomy. Specifically, the definition of the Mandelbrot set is

$$\mathcal{M} = \{c \,|\, Q_c^n(0) \not\to \infty\}$$

or, equivalently, by the Fundamental Dichotomy,

$$\mathcal{M} = \{c \,|\, K_c \text{ is connected}\}.$$

In Figure 2, we display the Mandelbrot set. The large cardioid-like region contains all c-vlaues for which Q_c admits an attracting fixed point. The value $c = 1/4$ lies at the cusp of this cardioid.

To summarize, we see that there really is a significant global consequence of the saddle-node bifurcation that occurs in the complex case when $c = 1/4$. Before the bifurcation ($-3/4 < c \leq 1/4$), the critical orbit tends to a fixed point, so K_c is connected. After the bifurcation ($c > 1/4$), the orbit of 0 tends to ∞ and so K_c shatters into infinitely many point components. Figure 3 shows this.

3 The "Complex" Complex Saddle-Node

Our goal in this section is to investigate the dynamical behavior of complex analytic maps near a more complicated saddle-node bifurcation. Specifically,

we will assume that, at the bifurcation parameter value, the neutral fixed point admits a non-degenerate homoclinic orbit. We will prove that, in the parameter space of such a family, there exist infinitely many copies of the Mandelbrot set. For parameter values which lie in these Mandelbrot sets, the corresponding maps admit invariant sets on which an iterate of the map is dynamically equivalent to the corresponding quadratic map.

To be specific, we consider a family of complex analytic maps given by

$$P_c(z) = z + c + z^2 + \cdots$$

which depends analytically on the complex parameter c. For convenience, we will assume that P_c is defined on the whole plane, but this restriction may be removed. When $c = 0$, this map has a fixed point at 0 with multiplier 1. We make two global assumptions about the dynamics of P_0. Our first assumption is that P_0 admits a non-degenerate homoclinic point (defined below). Our second assumption is that P_0 admits a unique critical point in the immediate basin of attraction of 0, and that this critical point is of order two. Our main result is then:

Theorem. *Under the above conditions, the parameter space for P_c (the c-plane) admits infinitely many subsets $\mathcal{M}_j$, $j > J$, which are homeomorphic to the standard Mandelbrot set $\mathcal{M}$ via a map $\phi_j : \mathcal{M}_j \to \mathcal{M}$ and which converge to 0. Moreover, for each $c \in \mathcal{M}_j$, there is a subset Λ_c of the Julia set of P_c on which some power of P_c is topologically conjugate to the map $z \mapsto z^2 + \phi_j(c)$ on its Julia set.*

In the case of a real polynomial, our assumptions are equivalent to the assumption that the graph of P_0 and one nearby P_c are as depicted in Figure **??**.

Fig. 1. The graphs P_0 and P_c

Note that P_0 admits a point z_0 whose orbit is both forward and backward asymptotic to the indifferent fixed point at 0. This is the *homoclinic orbit*. For P_c, the indifferent fixed point has disappeared, as has its basin of attraction. This allows orbits which previously tended to 0 to escape but then return to a neighborhood of 0. The resulting cyclic motion of orbits has been termed *intermittency* by Pomeau and Manneville [PM]. In this regard, our results can be interpreted as a description of the dynamical motions possible near intermittency.

Homoclinic points play a central role in smooth (non-analytic) dynamics. As is well known, the existence of a transverse homoclinic point for a map implies the existence of complicated orbit structure nearby (a Smale horseshoe–see [S]). An important question in dynamics is how this complicated behavior arises as a parameter is varied and a homoclinic point is "born." The results in this section give a partial answer to this question in the special case where the homoclinic point arises at the same time as a saddle-node bifurcation.

3.1 Dynamics of P_0

The local dynamical behavior of P_0 near 0 is well understood. Since $P_0'(0) = 1$, there is a neighborhood $\mathcal{O}$ of 0 in which the local inverse P_0^{-1} is well-defined. There also exist open disks D_- and D_+ in $\mathcal{O}$ which contain 0 in their boundary and satisfy

i. $P_0(D_-) \subset D_-$

ii. $P_0^{-1}(D_+) \subset D_+$

Moreover, each point in D_- has forward orbit which is asymptotic to 0, while each point in D_+ has forward orbit under P_0^{-1} which is asymptotic to 0.

D_- and D_+ may be chosen small enough so that $D_- - P_0(D_-)$ and $D_+ - P_0^{-1}(D_+)$ are fundamental domains for the dynamics of P_0 near 0. Using the map P_0, we may glue together the edges of $D_- - P_0(D_-)$ to form a cylinder which we denote by C_0^-. Using P_0^1, we may similarly construct C_0^+. C_0^- and C_0^+ are called Ecalle cylinders. See [DH1].

Let B_0 denote the immediate basin of attraction of 0 for P_0. It is known that B_0 is an open disk containing 0 in its boundary. It is also known that

the boundary of $B_0, \partial B_0$, lies in the Julia set of P_0 and that ∂B_0 is invariant under P_0. B_0 must contain at least one of the critical points of P_0. We will make the following simplifying assumption throughout:

Hypothesis A. $\overline{B}_0$ contains no asymptotic values of P_0 and exactly one critical point z_0 of P_0 which satisfies $P''(z_0) \neq 0$. Moreover, all other critical or asymptotic values of P are attracted to an attracting or a parabolic cycle.

The second part of Hypothesis A is included mainly for convenience and can be weakened significantly. From hypothesis A, it follows that $P|B_0$ is two-to-one, except at the critical value $P(z_0)$, which has only one preimage. Moreover, both z_0 and $P(z_0)$ lie in B_0, not on ∂B_0.

As a consequence of hypothesis A, it also follows that $P_0|\partial B_0$ is expanding. This follows in the polynomial case from [DH1, Part 2, X Proposition 3.] In the case of an entire map of finite type, this follows from results in [Mc]. Hence we may choose an open set B which contains $\overline{B}_0$ in its interior and which satisfies $P_0(B) \supset \overline{B}$. B is called an overflowing neighborhood of the immediate basin B_0.

3.2 Homoclinic Points

In this section we make a second assumption, more global in nature about the dynamics of P_0. A point $w \in D_+ - \overline{B}_0$ is called a homoclinic point if there exists $N > 0$ such that $P_0^N(w) \in B_0$. The orbit of w is therefore both forward and backward asymptotic to 0, with the backward orbit constructed using P_0^{-1}.

Let us assume that $P^i(w) \notin B_0 \cup D_+$ for $1 \leq i < N$. Then there is an open connected set U containing w and having the property that $P_0^N(U) = B$, where B is the overflowing neighborhood of B_0 constructed above. We say that w is a non-degenerate homoclinic point if $P_0^N \colon U \to B$ is an isomorphism.

We remark that it is entirely possible for some of the $P_0^i(U),\ 1 \leq i < N$ to contain critical points of P_0, in which case $P_0^N|U$ would not be one-to-one. In many cases, however, this assumption may be readily verified.

Our second main assumption about P_0 is: *Hypothesis B.* P_0 admits a non-degenerate homoclinic point. See Figure **??**.

Fig. 2

By adjusting D_+, we may assume that $U \subset D_+$ $P_0^{-1}(D_+)$. Hence it follows that $U_{-k} = P_0^{-k}(U)$ are disjoint open sets in $D_+ - B_0$ which tend to 0 as $k \to \infty$. See Figure **??**.

3.3 Ecalle cylinders for P_c

We may also erect Ecalle cylinders for P_c. By the results of [DH2], there is a wedge-shaped region $\mathcal{R}$ in the c-plane such that, if $c \in \mathcal{R}$, then P_c has a pair of repelling fixed points which we denote by $p_-(c)$ and $p_+(c)$. Moreover, we may choose Ecalle cylinders C_c^- and C_c^+ for each $c \in \mathcal{R}$ with vertices at $p_-(c)$ and $p_+(c)$. The $C_c^\pm$ may be chosen so that their boundaries depend continuously on c and tend to the boundaries of $C_0^\pm$ as $c \to 0$ in $\mathcal{R}$.

Let z_c denote the critical point of P_c in B. Without loss of generality, we may assume that the critical value $P_c(z_c) \subset C_c^-$.

As above, we may use the maps P_c and P_c^{-1} to glue together the boundaries of C_c^- and C_c^+. We choose the critical value as basepoint in C_c^- and any point in C_c^+ as basepoint. Then there are isomorphisms

$$\pi_c^-: C_c^- \to \mathbb{C}/\mathbb{Z}$$

$$\pi_c^+: C_c^+ \to \mathbb{C}/\mathbb{Z}$$

which take basepoints to 0.

Unlike the case when $c = 0$, there is a well defined transit map

$$\phi_c: C_c^- \to C_c^+$$

defined by

$$\phi_c(z) = P_c^k(z)$$

where k is the smallest positive integer for which $P_c^k(z) \in C_c^+$. Note that ϕ_c may be discontinuous. However, the projection of this map to $\mathbb{C}/\mathbb{Z}$ given by Φ_c, where

$$\Phi_c \circ \pi_c^-(z)\pi_c^+ \circ \phi_c(z)$$

is an isomorphism.

For $c \in \mathcal{R}$, there is also defined a map

$$\Phi: \mathcal{R} \to \mathbb{C}/\mathbb{Z}$$

given by

$$\Phi(c) = \Phi_c(P_c(z_c)) = \Phi_c(0)$$

The map Φ determines the image of the critical value in C_c^+ after it makes it transit between C_c^- and C_c^+. $\Phi(0)$ is not defined. However, according to [DH2], Theorem 16.11, Φ is given asymptotically by

$$\Phi(c) = \omega_0 + \frac{-2\pi}{\sqrt{c}} + o(1)$$

for some constant ω_0. Note that Φ wraps the wedge $\mathcal{R}$ infinitely often around $\mathbb{C}/\mathbb{Z}$ as $c \to 0$ in $\mathcal{R}$. In particular, if U is an open disk with compact closure in $\mathbb{C}/\mathbb{Z}$, then $\Phi^{-1}(\tilde{U})$ consists of infinitely many disjoint components V_j converging to 0 in $\mathcal{R}$ and on which Φ induces an isomorphism $V_j \to \tilde{U}$.

§4. **Polynomial like maps** In this section we recall some of the main results of [DH2]. Let D denote the closed disk. Suppose, for each $\lambda \in D$, there exists

i. open disks U_λ, U'_λ depending continuously on λ and satisfying $U_\lambda \subset U'_\lambda$.

ii. an analytic family of maps $F_\lambda \colon U_\lambda \to U'_\lambda$ depending analytically on λ with the property that $F_\lambda \colon U_\lambda \to U'_\lambda$ is of degree two. Any map with this property is said to be polynomial-like of degree 2.

iii. for each F_λ, there is a unique critical point $z_\lambda \in U_\lambda$. For $\lambda \in \partial D$, we assume that the map

$$\lambda \to F_\lambda(z_\lambda)$$

describes a curve in $U'_\lambda - U_\lambda$ which has winding number one with respect to each $z \in U_\lambda$. A family of maps with this property is said to have parametric degree one.

Any family of maps satisfying 1-3 is called a family of polynomial-like maps of degree two with parametric degree one.

A major result in [DH2, Theorem 4] asserts that such a family admits a subset $\mathcal{M} \subset \mathcal{D}$ which is homeomorphic to the standard Mandelbrot set via a map $c = c(\lambda)$. Moreover, for each $\lambda \in \mathcal{M}$, $\mathcal{F}_\lambda | \mathcal{U}_\lambda$ is topologically conjugate to $z \to z^2 + c(\lambda)$ on the filled Julia sets of each. That is, the dynamics of F_λ are equivalent to those of one of the quadratic maps $z \to z^2 + c$ on U_λ. Furthermore, this result asserts that all possible quadratic dynamical behavior occurs in the family F_λ.

3.4 Proof of the Theorem

Our goal in this section is to combine the results about Ecalle cylinders and parametrized families of analytic maps to prove that the maps P_c admit infinitely many copies of the Mandelbrot set $\mathcal{M}_{|,|} > \mathcal{J}$, in the region $\mathcal{R}$ in the c-plane.

Recall that there is an open set $U \subset D_+ - P_0^{-1}(D_+)$ with the property that

$$P_0^N : U \to B$$

is an isomorphism where B is an overflowing neighborhood of the immediate basin B_0 of 0. This follows from Hypothesis B. In particular, $P_0(B) \supset \overline{B}_0$. For c small enough, it follows that

$$P_c^N : U \to \mathbb{C}$$

is also an isomorphism. Moreover, if U_c is an open set sufficiently close to U, then $P_c^N | U_c$ is also an isomorphism, provided c is close enough to 0.

For each $j \in \mathbb{Z}^+$ sufficiently large, we will determine a subset V_j of $\mathcal{R}$ such that the family of maps P_c^{j+N+1} for $c \in V_j$ is a family of polynomial like maps of degree two with parametric degree one. Each of the V_j will be disjoint, and the $V_j \to 0$ as $j \to \infty$.

To construct V_j, recall that $U \subset C_0^+ - B_0$ is an open disk on which P_0^N is an isomorphism carrying U onto B. Let $\tilde{U} = \pi_0^+(U)$. $\tilde{U}$ is a disk in $\mathbb{C}/\mathbb{Z}$. By our remarks at the end of §3, $\Phi^{-1}(\tilde{U})$ consists of infinitely many components. These are the V_j. We may assume that the index j is chosen so that $c \in V_j$ implies that $P_c^{j+1}(z_c) \in C_c^+$, i.e., that j gives the "time" of transit of the critical point from C_c^- to C_c^+.

Let $U_c = (\pi_c^+)^{-1}(\tilde{U})$. For each c sufficiently small, P_c^N is an isomorphism which maps U_c onto an overflowing neighborhood of B.

Let $W_c = P_c^{-j}(U_c)$. Since $c \in V_j$, it follows that W_c contains the critical value of P_c. Now $P_c^j : W_c \to U_c$ is an isomorphism. Let $\tilde{W}_c$ denote the preimage of W_c containing z_c. $P_c | \tilde{W}_c$ is a degree two map onto W_c by hypothesis A. Note that, if c is sufficiently small, $\tilde{W}_c \subset B$. Therefore we have the fact that

$$P_c^{j+1+N} : \tilde{W}_c \to B$$

is a polynomial like map of degree two, if $c \in V_j$.

It remains to show that this family has parametric degree one. For this we first observe that $\Phi : V_j \to \tilde{U}$ is an isomorphism. So Φ maps ∂V_j to $\partial \tilde{U}$

with winding number one relative to the interior of $\tilde{U}$. If we lift this curve via $(\pi_c^+)^{-1}$, the result is still a degree one curve $c \to (\pi_c^+)^{-1} \circ \Phi(c)$ which is close to the boundary of U. Since P_c^N is C^0-close to P_0^N, it follows that, for $c \in \partial V_j$, $P_c^{j+1+N}(z_c)$ is a curve which wraps once around B_0. This completes the proof.

Remark. Much more can be said about the small copies of M: Each are "encaged" in "cauliflowers." These are collections of Cantor-like sets that nest down to $\mathcal{M}$. For more details, we refer to [DBDS].

4 Entire Functions

We now turn to some spectacular global bifurcations that occur in the dynamics of entire functions. Recall that an *entire function* is an analytic map $F : \mathbb{C} \to \mathbb{C}$ that is not a polynomial (and has no poles). Examples include the exponential family λe^z, the sine family $\lambda \sin z$, the cosine family $\lambda \cos z$, and the standard family $z + \omega + e \sin z$.

Since the function is entire, it follows that ∞ is not a superattracting fixed point. In this case ∞ is an essential singularity. Near ∞ the mapping possesses an extreme amount of "chaotic" behavior. By the great Picard Theorem, an entire function maps any neighborhood of ∞ onto the entire plane (missing at most one point), hitting each point infinitely often. This is an extreme case of sensitive dependence on initial conditions.

For the rest of this paper, we will concentrate on the exponential family $E_\lambda(x) = \lambda e^x$ where λ is real and nonzero. Much of what we discuss applies to other entire families as well. We will investigate again the saddle-node and period doubling bifurcation in this family. As in the quadratic polynomial case, these bifurcations will be quite tame in the real case, but incredibly "complex" in the complex case.

As in the quadratic family $Q_c(z) = z^2 + c$, it is the orbit of 0 that plays a crucial role in determining the dynamics of E_λ. For the exponential family, 0 is an asymptotic value rather than a critical point. A point z_0 is called an asymptotic value if there is a curve $\gamma(t)$ which tends to ∞ as $t \to t_0$ and whose image tends to z_0 as $t \to t_0$. Clearly, any curve tending to ∞ with real part tending to $-\infty$ has image that tends to 0 under E_λ.

As in quadratic dynamics, if E_λ admits an attracting cycle, then the orbit of 0 must tend to this cycle.

Unlike the quadratic case, we do not speak of the filled Julia set for the complex exponential. The reason is, as we show below, there are many parameter values for which the sets of points with bounded or unbounded orbits are both dense in the complex plane. It is more natural to speak about the Julia set, which we denote by $J(E_\lambda)$. For E_λ, there are three equivalent definitions of this set as

i) the closure of the set of repelling periodic points

ii) the set of points at which the family of functions E_λ^n fails to be a normal family in the sense of Montel

iii) the closure of the set of points whose orbits escape to ∞

The equivalence of i and ii is a classical fact; the equivalence of ii follows from results of Goldberg and Keen [GK].

There is an analogous Fundamental Dichotomy for complex exponentials. Again this dichotomy involves the orbit of 0, but this time it is somewhat more spectacular:

The Fundamental Dichotomy for Exponentials:
1. If $E_\lambda^n(0) \to \infty$, then the Julia set of E_λ is the entire plane.
2. If $E_\lambda^n(0) \not\to \infty$, then the Julia set contains Cantor bouquets and omits a half plane of the form $Re\, z < \nu$ for some $\nu \in \mathbb{R}$.

4.1 Bifurcation of Real Exponentials

The exponential family undergoes a saddle node bifurcation at $\lambda = 1/e$ since, when $\lambda = 1/e$, the graph of $E_{1/e}$ is tangent to the diagonal at 1. See Figure 4. We have $E_{1/e}(1) = 1$ and $E'_{1/e}(1) = 1$. When $\lambda > 1/e$, the graph of E_λ lies above the diagonal and all orbits (including 0) tend to ∞. When $\lambda < 1/e$, the graph of E_λ crosses the diagonal twice, at an attracting fixed point a_λ and a repeling fixed point r_λ. For later use note that $0 < a_\lambda < 1 < r_\lambda$. Note also that the orbit of 0 tends to a_λ. See Figure 4.

When $0 < \lambda < 1/e$, all points in the interval $-\infty < x < r_\lambda$ have orbits approaching the attracting fixed point. This changes when $\lambda > 1/e$, when all real orbits suddenly approach ∞. Thus we again have a global bifurcation on the real line at this saddle node point.

The exponential family also undergoes a period doubling bifurcation when $\lambda = -e$. Indeed, when $\lambda = -e$ we have a fixed point at -1 whose derivative

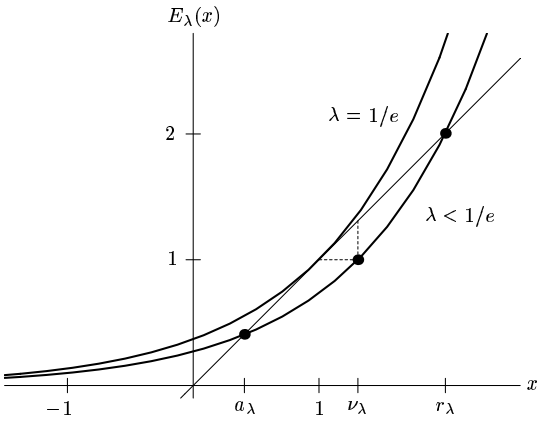

Figure 4: The graphs of E_λ for $\lambda = 1/e$ and $\lambda < 1/e$.

is -1. For $-e < \lambda < 0$, E_λ has an attracting fixed point on the negative real axis and all points on the real line tend to this fixed point. When $\lambda < -e$, it is easy to check that E_λ has an attracting 2-cycle and a repelling fixed point on the negative real axis, and all real orbits (except that of the fixed point) tend to the 2-cycle. Thus there is no real "global" bifurcation in this case.

4.2 The Complex Saddle Node Bifurcation for Exponentials

According to the Fundamental Dichotomy, when $0 < \lambda < 1/e$, the orbit of 0 does not escape to ∞. We will show in this section that, in this case, $J(E_\lambda)$ is a Cantor bouquet. When $\lambda > 1/e$, the orbit of 0 tends to ∞, and so $J(E_\lambda)$ is the entire plane.

In this section we will sketch the construction of a simple Cantor bouquet for the exponential map in the case where λ is real and satisfies $0 < \lambda \leq 1/e$. Much of the work in this chapter was done in collaboration with Clara Bodelon, Michael Hayes, Gareth Roberts, Lisa Goldberg, and John Hubbard [Bo].

In Figure 5, we display the Julia set for $E_{1/e}$. The complement of the Julia set is displayed in black. It appears that this Julia set contains large open sets, but this in fact is not the case. The Julia set actually consists of uncountably many curves or "hairs" extending to ∞ in the right half plane.

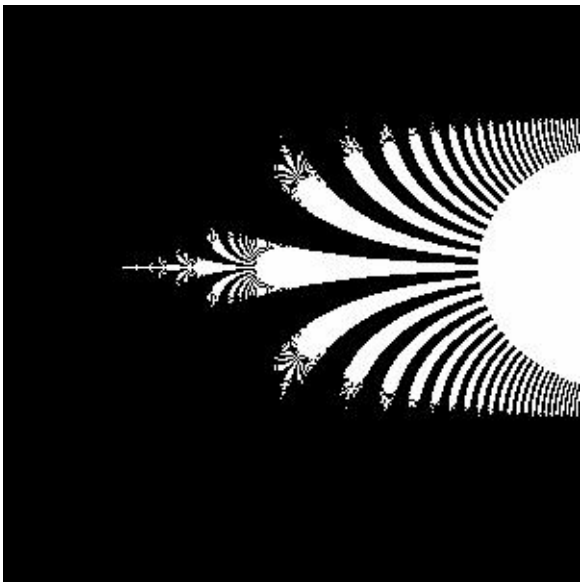

Figure 5: The Julia set for $\lambda = 1/e$.

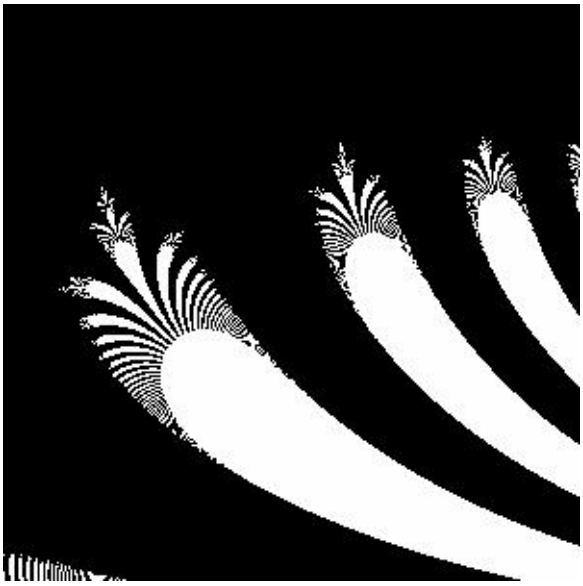

Figure 6: Magnification of the Julia set for $\lambda = 1/e$.

Each of the "fingers" in this Figure seems to have many smaller fingers protruding from them.

As we zoom in to this image, we see more and more of the self-similar structure, as each finger generates more and more fingers. In fact, each of these fingers consists of a cluster of hairs that are packed together so tightly that the resulting set has Hausdorff dimension 2 [McM].

4.3 The Idea of the Construction

Here is a rough idea of the construction of a Cantor bouquet. We will "tighten up" these ideas in ensuing sections.

For simplicity, we deal here only with $E(z) = (1/e)e^z$. As we have seen, E has a neutral fixed point at 1, on the real axis, and $E'(1) = 1$. The vertical line Re $z = 1$ is mapped to the circle of radius 1 centered at the origin. In fact, E is a contraction in the half plane H to the left of this line, since

$$|E'(z)| = \frac{1}{e} \exp(\text{Re}\, z) < 1$$

if $z \in H$. Consequently, all points in H have orbits that tend to 1. Hence this half plane lies in the complement of the Julia set. We will try to paint the picture of the Julia set of E by painting instead its complement, the stable set.

Since the half plane H is forward invariant under E, we can obtain the entire stable set by considering all preimages of this half plane. Now the first preimage of H certainly contains the horizontal lines Im $z = (2k+1)\pi$, Re $z \geq 1$, for each integer k, since E maps these lines to the negative real axis which lies in H. Hence there are open neighborhoods of each of these lines that lie in the stable set. The first preimage of H is shown in Figure 7. The complement of $E^{-1}(H)$ consists of infinitely many "fingers." The fingers are $2k\pi i$ translates of eachother, and each is mapped onto the complementary half plane Re $z \geq 1$.

We denote the fingers in the complement of $E^{-1}(H)$ by C_j with $j \in \mathbb{Z}$, where C_j contains the half line Im $z = 2j\pi$, Re $z \geq 1$, which is mapped into the positive real axis. That is, the C_j are indexed by the integers in order of increasing imaginary part. Note that C_j is contained within the strip $-\frac{\pi}{2} + 2j\pi \leq \text{Im}\ z \leq \frac{\pi}{2} + 2j\pi$.

Now each C_j is mapped in one-to-one fashion onto the entire half plane Re $z \geq 1$. Consequently each C_j contains a preimage of each plane Re $z \geq 1$.

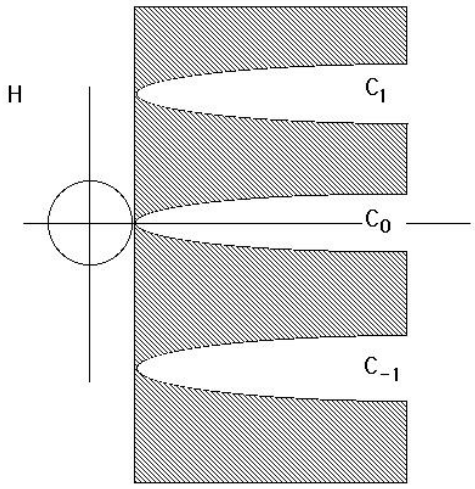

Figure 7: The preimage of H consists of H and the shaded region.

Consequently each C_j contains a preimage of each other C_k. Each of these preimages forms a subfinger which extends to the right in the half plane H. See Figure 8. The complement of these subfingers necessarily lies in the stable set.

Now we continue inductively. Each subfinger is mapped onto one of the original fingers by E. Consequently, there are infinitely many sub-sub-fingers which are mapped to the C_j's by E^2. So at each stage we remove the complement of infinitely many subfingers from each remaining finger.

After performing this operation infinitely many times, we do not end up with points. Rather, the intersection of all of these fingers is a simple curve extending to ∞.

This collection of curves forms the Julia set. E permutes these curves and each curve consists of a well-defined endpoint together with a "hair" which extends to ∞. It is tempting to think of this structure as a "Cantor set of curves," i.e., a product of the set of endpoints and the half-line. However, this is not the case as the set of endpoints is not closed.

Note that we can assign symbolic sequences to each point on these curves. We simply watch which of the C_j's these orbit of the point lies in after each iteration and assign the corresponding index j. That is, to each hair in the Julia set we attach an infinite sequence $s_0 s_1 s_2 \ldots$ where $s_j \in \mathbb{Z}$ and $s_j = k$

Figure 8: The second preimage of H in one of the fingers C_j.

if the j^{th} iterate of the hair lies in C_j. The sequence $s_0 s_1 s_2 \ldots$ is called the *itinerary* of the curve.

For example, the portion of the real line $\{x \mid x \geq 1\}$ lies in the Julia set since all points (except 1) tend to ∞ under iteration, not to the fixed point.

This points up a fact that makes entire dynamics very different from polynomial dynamics. The hair $\{x \mid x > 1\}$ lies in $J(E)$ despite the fact that these orbits go to ∞. The difference is the fact that ∞ is an essential singularity for E, not a superattracting fixed point. Another temptation is to say that there is a hair corresponding to every sequence $s_0 s_1 s_2 \ldots$ This, unfortunately, is not true either, as certain sequences simply grow too quickly to correspond to orbits of E. See Deville [**?**] for more details.

So this is $J(E)$: a "hairy" object extending toward ∞ in the right-half plane. We call this object a *Cantor bouquet*. We will see that this bouquet has some rather interesting topological properties as we investigate further.

4.4 Cantor N-Bouquets

In this section we begin the construction of a Cantor bouquet. We first construct a Cantor set on which E_λ is conjugate to the shift map on $2N+1$ symbols.

The graph of E_λ (see Figure 4) shows that E_λ has two fixed points on the real axis, an attracting fixed point at q_λ and a repelling fixed point at

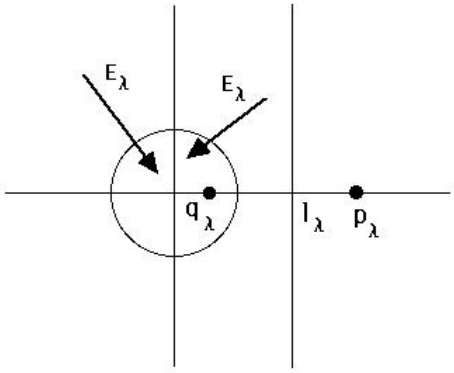

Figure 9: E_λ maps the half plane $\operatorname{Re} z < \ell_\lambda$ inside the disk.

p_λ, with $0 < q_\lambda < p_\lambda$. Note that $q_\lambda < -\log\lambda < p_\lambda$ since

$$E'_\lambda(q_\lambda) < 1 = E'_\lambda(-\log\lambda) < E'_\lambda(p_\lambda).$$

Fix a real number ℓ_λ satisfying $-\log\lambda < \ell_\lambda < p_\lambda$ and observe that, if $\operatorname{Re} z \geq \ell_\lambda$, then

$$|E'_\lambda(z)| = \lambda e^{\operatorname{Re} z} \geq \lambda e^{\ell_\lambda} > \mu > 1$$

for some constant $\mu > 1$. Thus E_λ is "expanding" in the half plane $\operatorname{Re} z \geq \ell_\lambda$.

Note that E_λ maps the half plane $\operatorname{Re} z < \ell_\lambda$ inside itself, in fact to the circle of radius $E_\lambda(\ell_\lambda)$ centered at 0, since $E_\lambda(\ell_\lambda) < \ell_\lambda$. Now E_λ has a fixed point in this half plane, namely q_λ. See Figure 9 It follows from the Corollary to the Schwarz lemma that all orbits in this half plane tend to q_λ, and so the Julia set of E_λ is contained in the right-half plane $\operatorname{Re} z \geq \ell_\lambda$.

We will now construct a collection of invariant Cantor sets for E_λ in the right-half plane $\operatorname{Re} z \geq \ell_\lambda$ on which the dynamics of E_λ is conjugate to the one-sided shift map on $2N+1$ symbols. Fix an integer $N \geq 1$. Consider the rectangle B_N bounded as follows:

1. On the left by $\operatorname{Re} z = \ell_\lambda$
2. Above and below by $\operatorname{Im} z = \pm(2N+1)\pi$
3. On the right by $\operatorname{Re} z = r_\lambda$ where r_λ satisfies $\lambda e^{r_\lambda} > r_\lambda + (2N+1)\pi$

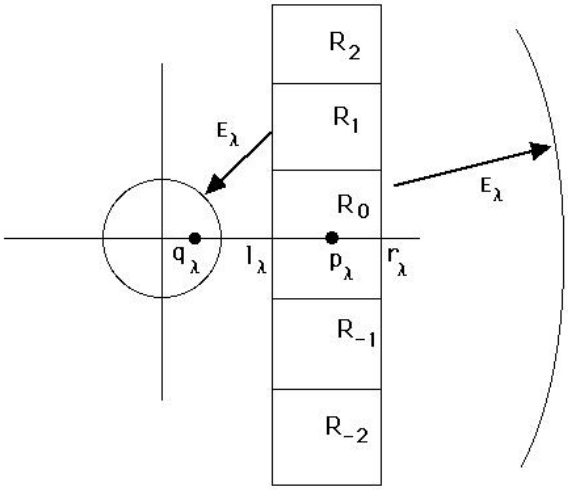

Figure 10: Construction of the R_i

The inequality in part 3 guarantees that E_λ maps the right-hand edge of the rectangle to a circle of radius λe^{r_λ} centered at 0 which contains the entire rectangle B_N in its interior. Note also that E_λ maps B_N onto the annular region $\{z \mid \lambda e^{\ell_\lambda} \leq |z| \leq \lambda e^{r_\lambda}\}$ and that B_N is contained in the interior of this annulus.

For each integer i with $-N \leq i \leq N$, consider the subrectangle $R_i \subset B_N$ defined by $\ell_\lambda \leq \text{Re } z \leq r_\lambda$ and $(2i-1)\pi \leq \text{Im } z \leq (2i+1)\pi$. Note that E_λ maps each R_i onto the annular region above, and that $|E'_\lambda(z)| > \mu > 1$. Moreover, if we restrict E_λ to the interior of R_i we obtain an expanding analytic isomorphism which maps the interior of R_i onto a region that covers all of B_N. See Figure 10. As a consequence, we may define an analytic branch of the inverse of E_λ, $L_{\lambda,i}$, which takes B_N into R_i for each i. Clearly, $L_{\lambda,i}$ is a contraction for each i. In particular, there is a constant $\nu < 1$ such that $|L_{\lambda,i}| < \nu$ for all i and all z in B_N. See Figure 10.

Now define

$$\Lambda_N = \{z \in B_N | E^j_\lambda(z) \in B_N \text{ for } j = 0, 1, 2, \ldots\},$$

that is, Λ_N is the set of points whose orbits remain for all time in B_N. Let Σ_N denote the space of infinite sequences $s = (s_0 s_1 s_2 \ldots)$ where each s_j is an integer, $-N \leq s_j \leq N$. Endow Σ_N with the product topology. For each

Figure 11: Just a blank figure, sorry.

$s \in \Sigma_N$, we identify a unique point in Λ_N via

$$\phi(s) = \lim_{n \to \infty} L_{\lambda,s_0} \circ L_{\lambda,s_1} \circ \cdots \circ L_{\lambda,s_n}(z)$$

where z is any point in B_N. The fact that $\phi(s)$ is a unique point follows from the fact that each L_{λ,s_i} is a contraction in B_N. In fact $\phi(s)$ is independent of z, and ϕ defines a homeomorphism between Σ_N and Λ_N. Moreover, ϕ gives a conjugacy between the shift map on the sequence space Σ_N and $E_\lambda|\Lambda_N$.

Since $|E'_\lambda(z)| > \mu > 1$ for all $z \in \Lambda_N$, it follows that Λ_N is a hyperbolic set, and so $\Lambda_N \subset J(E_\lambda)$. Moreover, we have an increasing sequence of these Cantor sets $\Lambda_1 \subset \Lambda_2 \subset \ldots$. Since each point in Λ_N lies in the complement of the basin of attraction of q_λ, it follows that $\Lambda_N \subset J(E_\lambda)$. We have proved:

Theorem 4.1 *Suppose $0 < \lambda < 1/e$. Then the set of points Λ_N whose orbit remains for all time in the rectangle B_N is a Cantor set in $J(E_\lambda)$. The action of E_λ on this Cantor set is conjugate to the shift map on $2N+1$ symbols.*

We next claim that each point $z_s = \phi(s)$ in one of the Λ_i comes with a unique "hair" attached. This hair is a curve associated with a natural parametrization

$$h_{\lambda,s}\colon [1, \infty) \to \mathbb{C}$$

that satisfies

1. $h_{\lambda,s}(1) = z_s$
2. $h_{\lambda,s}$ is a homeomorphism
3. If $t \neq 1$, then Re $E_\lambda^n(h_{\lambda,s}(t)) \to \infty$ as $n \to \infty$
4. For each t, $h_{\lambda,s}(t)$ lies in the horizontal strip
$$(2s_0 - 1)\pi < \text{Im } z < (2s_0 + 1)\pi$$
5. $E_\lambda(h_{\lambda,s}(t)) = h_{\lambda,\sigma(s)}(E_{1/e}(t))$ where $\sigma(s)$ denotes the shift applied to the sequence s.

By condition 4, the orbit of $h_{\lambda,s}(t)$ tends to ∞. Hence this point does not lie in the basin of attraction of q_λ and as a conseqeunce each point on a hair lies in the Julia set.

To define $h_{\lambda,s}$, recall that $E_{1/e}$ has a unique fixed point at 1 and that $E_{1/e}\colon [1,\infty) \to [1,\infty)$. If $t > 1$, then $E_{1/e}^n(t) \to \infty$ as $n \to \infty$. Recall that L_{λ,s_i} is the branch of the inverse of E_λ which now takes values in the horizontal strip given by

$$(2s_i - 1)\pi \leq \text{Im } z \leq (2s_i + 1)\pi.$$

Then define

$$h_{\lambda,s}(t) = \lim_{n\to\infty} L_{\lambda,s_0} \circ \ldots \circ L_{\lambda,s_{n-1}}(E_{1/e}^n(t)).$$

It can be shown that $h_{\lambda,s}$ has all of the properties listed above.

Thus, for each $N \geq 1$, we have a map

$$H_\lambda\colon \Sigma_N \times [0,\infty 0 \to \mathbb{C}.$$

This map is also a homeomorphism. We call the image of H_λ a *Cantor N-bouquet* and denote it by $\mathcal{B}_{\lambda,N}$.

These Cantor N-bouquets form the skeleton of the Julia set. Indeed, every repelling periodic point has bounded itinerary, and hence lies in some $\mathcal{B}_{\lambda,N}$ for some N. In particular, such a point lies at the endpoint of a hair in some Cantor N-bouquet (and hence any M-bouquet for $M > N$). This means that the N-bouquets are dense in the Julia set. So

$$J(E_\lambda) = \text{ Closure of } \cup_{N=1}^\infty \mathcal{B}_{\lambda,N}.$$

We call the closure of the union of the N-bouquets a *Cantor bouquet.*

Now there are points in the Cantor bouquet that do not lie in $\mathcal{B}_{\lambda,N}$ for any N. Indeed, there are many points whose itineraries are unbounded. To understand these points, we need to introduce the notion of a straight brush. This is the topic of the following section.

4.5 Straight Brushes

To describe the structure of a Cantor bouquet, we introduce the notion of a *straight brush.*

To each irrational number ζ, we assign an infinite string of integers $n_0 n_1 n_2 \ldots$ as follows. We will break up the real line into open intervals $I_{n_0 n_1 \ldots n_k}$ which have the following properties

1. $I_{n_0 \ldots n_k} \supset I_{n_0 \ldots n_{k+1}}$.
2. The endpoints of $I_{n_0 \ldots n_k}$ are rational.
3. $\zeta = \bigcap_{k=1}^{\infty} I_{n_0 \ldots n_k}$

Now there are many ways to do this. We choose the following method based on the Farey tree. Inductively, we first define $I_k = (k, k+1)$. Given $I_{n_0 \ldots n_k}$ we define $I_{n_0 \ldots n_k j}$ as follows. Let

$$I_{n_0 \ldots n_k} = \left(\frac{\alpha}{\beta}, \frac{\gamma}{\delta} \right).$$

Let $p_0/q_0 = (\alpha + \gamma)/(\beta + \delta)$, the Farey child of α/β and γ/δ. Let p_n/q_n be the Farey child of p_{n-1}/q_{n-1} and γ/δ for $n > 0$, and let p_{n-1}/q_{n-1} be the Farey child for α/β and p_n/q_n for $n \geq 0$. We then set $I_{n_0 \ldots n_k j}$ to be the open interval $(p_j/q_j, p_{j+1}/q_{j+1})$.

Example. $I_0 = (0, 1)$. The Farey child of $0/1$ and $1/1$ is $1/2$, so $p_0/q_0 = 1/2$. Then $p_1/q_1 = \frac{1}{2} \oplus \frac{1}{1} = 2/3$, $p_2/q_2 = \frac{2}{3} \oplus \frac{1}{1} = \frac{3}{4}$, and $p_n/q_n = n+1/n+2$ for $n > 0$.

For the remaining n we have

$$p_{-1}/q_{-1} \quad = \quad \frac{0}{1} \oplus \frac{1}{2} = \frac{1}{3}$$

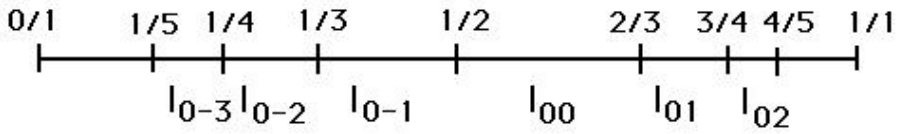

Figure 12: Construction of I_{0n}.

$$\begin{aligned} p_{-2}/q_{-2} &= \frac{0}{1} \oplus \frac{1}{3} = \frac{1}{4} \\ p_{-n}/q_{-n} &= \frac{1}{n+2}. \end{aligned}$$

Therefore, if $n \geq 0$,

$$I_{0n} = \left(\frac{n+1}{n+2}, \frac{n+2}{n+3}\right)$$

and if $n < 0$,

$$I_{0n} = \left(\frac{1}{-n+2}, \frac{1}{-n+1}\right).$$

See Figure 12. Note that we exhaust all of the rationals via this procedure, so each irrational is contained in a unique $I_{n_0 n_1 \ldots}$.

We now define a straight brush, a notion due to Aarts and Oversteegen [AO].

Definition 4.2 *A straight brush B is a subset of $[0,\infty) \times \mathcal{N}$, where $\mathcal{N}$ is a dense subset of irrationals. B has the following 3 properties.*

1. *B is "hairy" in the following sense. If $(y,\alpha) \in B$, then there exists a $y_\alpha \leq y$ such that $(t,\alpha) \in B$ iff $t \geq y_\alpha$. That is the "hair" (t,α) is contained in B where $t \geq y_\alpha$. y_α is called the endpoint of the hair corresponding to α.*

2. *Given an endpoint $(y_\alpha,\alpha) \in B$ there are sequences $\beta_n \uparrow \alpha$ and $\gamma_n \downarrow \alpha$ in $\mathcal{N}$ such that $(y_{\beta_n},\beta_n) \to (y_\alpha,\alpha)$ and $(y_{\gamma_n},\gamma_n) \to (y_\alpha,\alpha)$. That is, any endpoint of a hair in B is the limit of endpoints of other hairs from both above and below.*

3. B is a closed subset of $\mathbb{R}^2$.

Exercise. For any rational number v and any sequence of irrationals $\alpha_n \in \mathcal{N}$ with $\alpha_n \to v$, show that the hairs $[y_{\alpha_n}, \alpha_n]$ must tend to $[\infty, v]$ in $[0, \infty) \times \mathbb{R}$.

Exercise. Show that condition 2 above may be changed to: if (y, α) is any point in B (y need not be the endpoint of the α-hair), then there are sequences $\beta_n \uparrow \alpha$, $\gamma_n \downarrow \alpha$ so that $(y_{\beta_n}, \beta_n) \to (y, \alpha)$ and $(y_{\gamma_n}, \gamma_n) \to (y, \alpha)$ in B.

Remark. Let $(y, \alpha) \in B$ and suppose y is not the endpoint y_α. Then one may prove that (y, α) is inaccessible in $\mathbb{R}^2$ in the sense that there is no continuous curve $\gamma : [0, 1] \to \mathbb{R}^2$ such that $\gamma(t) \notin B$ for $0 \leq t < 1$ and $\gamma(1) = (y, \alpha)$. One may also prove that (y_α, α) is accessible in $\mathbb{R}^2$.

THese exercises show that a straight brush is a remarkable object from the topological point of view. Let's view a straight brush as a subset of the Riemann sphere and set $B^* = B \cup \infty$, i.e., the straight brush with the point at infinity added. Let $\mathcal{E}$ denote the set of endpoints of B, and let $\mathcal{E}^* = \mathcal{E} \cup \infty$. Then we have the following result, due to Mayer [Ma]:

Theorem 4.3 *The set $\mathcal{E}^*$ is a connected set, but $\mathcal{E}$ is totally disconnected.*

That is, the set $\mathcal{E}^*$ is a connected set, but if we remove just one point form this set, the resulting set is totally disconnected. Topology really is a weird subject!

The reason for this is that, if we draw the straight line in the plane (γ, t) where γ is a fixed rational, and then we adjoin the point at infinity, we find a disconnection of $\mathcal{E}$. This, however, is not a disconnection of $\mathcal{E}^*$. Moreover, the fact that any non-endpoint in B is inaccessible shows that we cannot disconnect $\mathcal{E}^*$ by any other curve.

Remark. Aarts and Oversteegen have shown that any two straight brushes are ambiently homeomorphic, i.e., there is a homeomorphism of $\mathbb{R}^2$ taking one brush onto the other. This leads to a formal definition of a Cantor bouquet.

Definition 4.4 *A Cantor bouquet is a subset of $\overline{\mathbb{C}}$ that is homeomorphic to a straight brush (with ∞ mapped to ∞).*

Our main goal in this section is to sketch a proof of the following result:

Theorem 4.5 *Suppose $0 < \lambda < 1/e$. Then $J(E_\lambda)$ is a Cantor bouqet.*

Proof. To construct the homeomorphism between the brush and $J(E_\lambda)$ we first introduce symbolic dynamics. Recall that E_λ has a repelling fixed point $p_\lambda > 0$ in $\mathbb{R}$ and that the half plane $\operatorname{Re} z < p_\lambda$ lies in the stable set. Similarly the horizontal strips

$$\frac{\pi}{2} + 2k\pi < \operatorname{Im} z < \frac{\pi}{2} + (2k+1)\pi$$

are contained in the stable set since E_λ maps these strips to $\operatorname{Re} z < 0$ which is contained in $\operatorname{Re} z < p_\lambda$.

We denote by S_k the closed halfstrip given by

$$\operatorname{Re} z \geq p_\lambda \text{ and } -\frac{\pi}{2} + 2k\pi \leq \operatorname{Im} z \leq \frac{\pi}{2} + 2k\pi.$$

Note that these strips contain the Julia set since the complement of the strips lies in the stable set.

Given $z \in J(E_\lambda)$, we define the itinerary of z, $S(z)$, as usual by

$$S(z) = s_0 s_1 s_2 \dots$$

where $s_j \in \mathbb{Z}$ and $s_j = k$ iff $E_\lambda^j(z) \in S_k$. Note that $S(z)$ is an infinite string of integers that indicates the order in which the orbit of z visits the S_k. We will associate to z the irrational number given by the itinerary of z (and the decomposition of the irrationals described above). This will determine the hair in the straight brush to which z is mapped. See Figure 13. Thus we need only define the y-value along this hair. This takes a little work.

We will construct a sequence of rectangles $R_k(j)$ for each $j, k \geq 0$. The point $E_\lambda^j(z)$ will be contained in $R_k(j)$ for each $k \geq 0$. And we will have $R_{k+1}(j) \subset R_k(j)$ for each j and k. Each $R_k(j)$ will have sides parallel to the axes and be contained in a strip S_α. Finally each $R_k(j)$ will have height π. Since the $R_k(j)$ are nested with respect to k, the intersection $\bigcap_{k=0}^{\infty} R_k(j)$ will be a nonempty rectangle of height π that contains $E_\lambda^j(z)$. We then define $h(z)$ to be the real part of the left hand edge of this limiting rectangle.

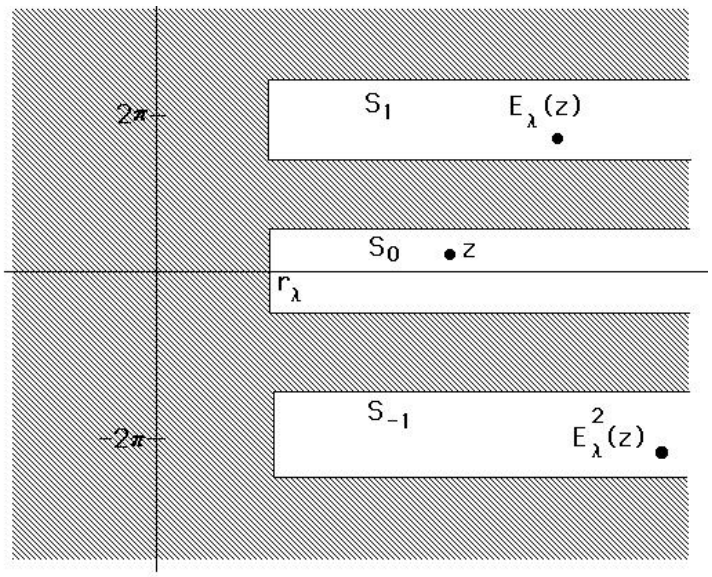

Figure 13: The itinerary of z is $0, 1, -1, \ldots$.

To begin the construction, we set $R_0(j)$ to be the square centered horizontally at $E_\lambda^j(z)$ with sidelength π and contained in the appropriate strip S_α. Observe that $E_\lambda(R_0(j)) \supset R_0(j+1)$. Indeed, the image of $R_0(j)$ is an annulus whose inner radius is $e^{-\pi/2}|E_\lambda^{j+1}(z)|$ and outer radius $e^{\pi/2}|E_\lambda^{j+1}(z)|$. Now $e^{\pi/2} > 4$ and $e^{-\pi/2} < 1/4$ so the image annulus is much larger than $R_0(j+1)$. See Figure 14.

It follows that we may find a narrower rectangle $R_1(j)$ strictly contained in $R_0(j)$ having the property that the height of $R_1(j)$ is π and the image $E_\lambda(R_1(j))$ just covers $R_0(j+1)$. That is, $R_1(j)$ is the smallest rectangle in $R_0(j)$ whose image annulus is just wide enough so that $R_0(j+1)$ fits inside. See Figure 15. Note that $E_\lambda^j(z) \in R_1(j)$.

Continue inductively by setting $R_k(j)$ to be the subrectangle of $R_{k-1}(j)$ whose image just covers $R_{k-1}(j+1)$. The $R_k(j)$ are clearly nested for each fixed j.

Example. Suppose $z = p_\lambda$. We have that $R_0(j)$ is the square bounded by $\mathrm{Re}\ z = p_\lambda \pm \pi/2$ and $\mathrm{Im}\ z = \pm\pi/2$ for each j. One may check that, for each j, $\bigcap_{k=0}^{\infty} R_k(j)$ is the strip bounded by $\mathrm{Re}\ z = p_\lambda$ and $\mathrm{Re}\ z = \zeta$ where the circle of radius λe^ζ passes through $\zeta \pm i\pi/2$. See Figure 16.

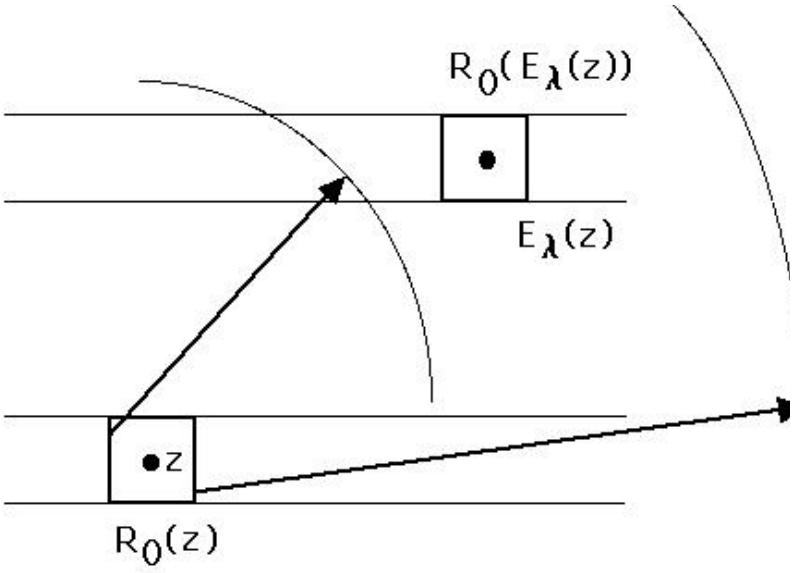

Figure 14: Construction of $R_0(0)$ and $R_0(1)$.

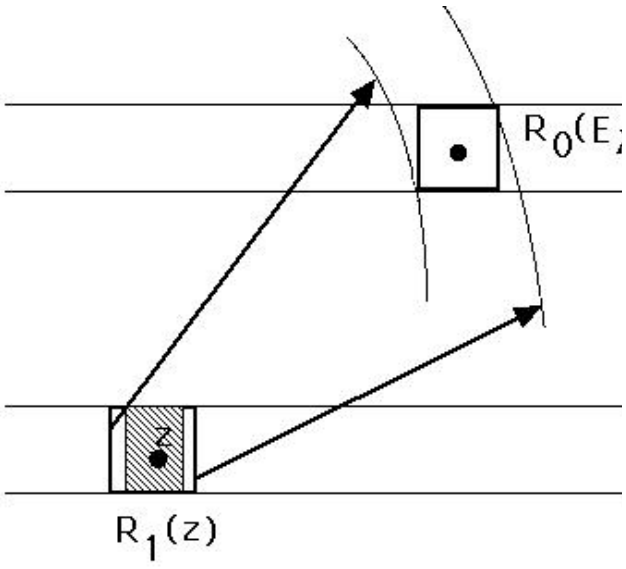

Figure 15: Construction of $R_1(0)$.

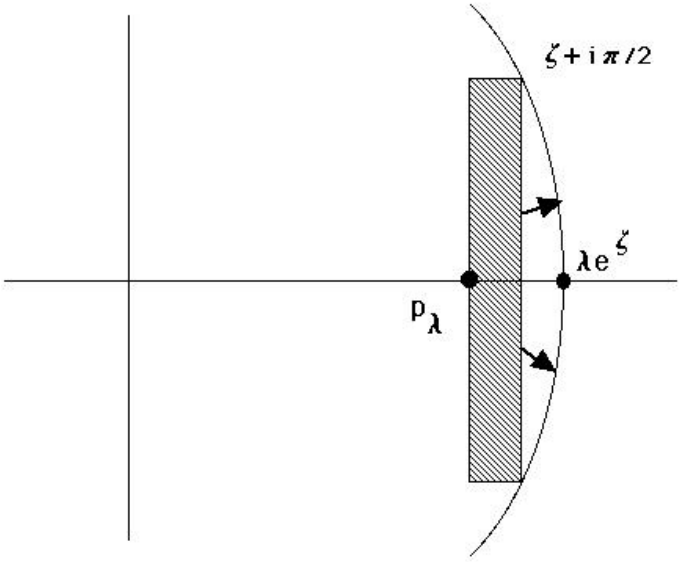

Figure 16: The intersection of $R_j(0)$.

Suppose z has itinerary $S(z) = s_0 s_1 s_2 \ldots$. Let $I(S(z))$ denote the irrational number determined by the sequence $S(z)$ as above. Then set $\phi(z) = (h(z), I(S(z)))$. We claim that ϕ is a homeomorphism onto a straight brush. For a proof, we refer to [AO]

4.6 Connectedness Properties of Cantor Bouquets

We call the set of endpoints of a Cantor bouquet the *crown*. Since a Cantor bouquet is homeomorphic to a straight brush with the points at ∞ coinciding, it follows that any Cantor bouquet has the amazing connectedness property that the crown together with ∞ is connected, but the crown alone is totally disconnected.

It can be shown that the construction above works for any exponential for which there exists an attracting or neutral periodic point. However, in the general case, some of the hairs in the Cantor bouquet may be attached to the same point in the crown. See [BD].

McMullen [McM] has shown that the Hausdorff dimension of the Cantor bouquet constructed above is 2 but its Lebesgue measure is zero. This

accounts for why figures 5 and 6 seem to have open regions in the Julia set.

Cantor bouquets arise in many critically finite entire maps. In order to see this, suppose all singular points of F lie in some disk B_r of radius r centered at the origin. Consider the preimage $F^{-1}(\mathbf{C} - B_r)$ and let U be any component of this set. Now F maps U analytically onto $C - B_r$ without singular values, so F must be a universal covering. As such, F acts like an exponential map. If, in fact, U is disjoint from $\mathbf{C} - B_r$ and F has sufficient growth in U, it can be shown (see [DT]) that there is an invariant Cantor bouquet for F in U. For a specific example dealing with the complex standard map $z \mapsto z + \omega + \epsilon \sin z$ we refer to [Fa].

Remark. One may construct a similar Cantor bouquet for the map $S_\lambda(z) = \lambda \sin z$ when $0 < \lambda < 1$. In this case, the rectangles will now be arranged vertically and there will be two bouquets: one in the upper half plane and one in the lower.

4.7 Uniformization of the Attracting Basin

The basin of attraction Ω_λ of E_λ is an open, dense, and simply connected subset of the Riemann sphere. Hence the Riemann Mapping Theorem guarantees the existence of a uniformization $\phi_\lambda \colon D \to \Omega_\lambda$. Given such a uniformization, it is natural to ask if the uniformizing map extends to the boundary of D.

In order to extend ϕ_λ to the boundary, we need that the image of a straight ray $re^{i\theta}$ where θ is constant under ϕ_λ converge to a single point as $r \to 1$. It is known that if the boundary of the uniformizing region is locally connected, then in fact ϕ_λ does extend continuously to D. On the other hand, if the boundary of the region is not locally connected, then not all rays need converge (though a full measure set of them must converge). In our case, the boundary of Ω_λ is nowhere locally connected (except at ∞). However, it is a fact that all rays do converge. In fact, they land at precisely the endpoints of the Cantor bouquet. This means that we can induce a map on the set of endpoints, but that map is necesarily nowhere continuous [Pi].

In the case of a straight brush, it is clear that all rays do land at the crown of the bouquet. A direct proof for E_λ is given in [DG].

Remark. It can be shown that if we normalize the Riemann map ϕ_λ so that 0 is mapped to 0, then the induced map $\phi_\lambda^-1 \circ E_\lambda \circ \phi_\lambda$ on the unit disk is given by

$$T_\mu(z) = \exp\left(i\left(\frac{\mu + \overline{\mu}}{1 + z}\right)\right).$$

Here μ is a parameter that lies in the upper half plane and depends upon λ.

4.8 After the Bifurcation

As we have seen, when $\lambda > 1/e$, the Julia set of E_λ is the entire plane. In this appendix, we consider the case $\lambda = 1$ and write simple $E(z) = e^z$. In 1981, Misiurewicz showed that $J(E) = \mathbf{C}$, answering a sixty-year-old question of Fatou. We present his proof of this fact below.

The following proposition highlights one of the differences between $E(z)$ and polynomials: points which tend to ∞ under iteration of E need not be in the stable set.

Proposition 4.6 *The real line is contained in $J(E)$.*

Proof. Let S denote the strip $|\text{Im }(z)| \leq \pi/3$. If $z = x + iy \in S$, then since $|e^x \cos y| \geq e^x/2 > x$, it follows that $E(z)$ lies to the right of z. The last inequality follows since $\frac{1}{2} > \frac{1}{e}$. In particular, if $E^i(z) \in S$ for all i, we have $\text{Re}\, E^i(z) \to \infty$.

If $z \in S$ with $\text{Re }(z) > 1$ and $\text{Im }(z) \neq 0$, then we also have

$$|e^x \sin y| > e^x(\frac{2}{\pi}|y|) > |y|.$$

Consequently, if $z \in S$ but $z \notin \mathbf{R}$, and if $\text{Re}\, z > 1$, then $|\text{Im }(E^i(z))|$ must grow as i increases. Hence there exists $j > 0$ for which $E^j(z) \notin S$. Thus all points in S which do not lie in $\mathbf{R}$ must eventually leave S.

Now let U be any neighborhood of $x \in \mathbf{R}$. Recall that $E^j(x) \to \infty$. By the above remarks, there is $N > 0$ such that, for each $j > N$, $E^j(U)$ intersects both $\mathbf{R}$ and the line $y = \pi/3$ at points with real part > 1. Consequently, $E^{j+1}(U)$ meets both $\mathbf{R}$ and $y = \pi$, since $y = \pi/3$ is mapped to the ray $\theta = \pi/3$. Hence $E^{j+2}(U)$ meets the negative real axis, and so a portion of U is mapped by E^{j+3} inside the unit disk. Thus, for sufficiently large j, there are points z_1 and z_2 in U for which $E^j(z_1)$ lies in the unit disk and for which $|E^j(z_2)|$ is arbitrarily large. It follows that $\{E^n\}$ is not normal in U, and so $x \in J(E)$.

□

Thus to show that $J(E) = \mathbf{C}$, it suffices to show that inverse images of the real line are dense in $\mathbf{C}$. For this, we need several lemmas.

Lemma 4.7 $|\text{Im }(E^n(z))| \leq |(E^n)'(z)|$.

Proof. If $z = x + iy$, we have

$$\begin{aligned} |\text{Im } (E(z))| &= e^x |\sin y| \\ &\leq e^x |y| \\ &= |E'(z)||\text{Im } (z)| \end{aligned}$$

so that

$$\frac{|\text{Im } (E(z))|}{|\text{Im } (z)|} \leq |E'(z)|$$

if $z \notin \mathbf{R}$. More generally, if $E^n(z) \notin \mathbf{R}$, we may apply this inequality repeatedly to find

$$\begin{aligned} \frac{|\text{Im } (E^n(z))|}{|\text{Im } (E(z))|} &= \prod_{i=1}^{n-1} \frac{|\text{Im } E(E^i(z))|}{|\text{Im } (E^i(z))|} \\ &\leq \prod_{i=1}^{n-1} |E'(E^i(z))|. \end{aligned}$$

Since $|\text{Im } (E(z))| \leq |E(z)| = |E'(z)|$ we may write

$$\begin{aligned} |\text{Im } (E^n(z))| &\leq \prod_{i=0}^{n-1} |E'(E^i(z))| \\ &= |(E^n)'(z)|. \end{aligned}$$

□

The proof of Proposition 4.6 shows that most points must leave the strip S under iteration. The next lemma shows, however, that most points must eventually return.

Lemma 4.8 *Let U be an open connected set. Then only finitely many of the $E^n(U)$ can be disjoint from S.*

Proof. Let us assume that infinitely many of the images of U are disjoint from S. If there is an n for which E^n is not a homeomorphism taking U onto its image, then there exist $z_1, z_2 \in U$, $z_1 \neq z_2$, for which $E^n(z_1) = E^n(z_2)$. Consequently, there is a j for which $E^j(z_1) = E^j(z_2) + 2k\pi i$ for some $k \in \mathbf{Z} - \{0\}$. But then $E^j(U)$ must meet a horizontal line of the form $y = 2m\pi$ for $m \in \mathbf{Z}$ and so $E^{j+1}(U)$ meets $\mathbf{R}$. Hence $E^{j+\alpha}(U)$ meets $\mathbf{R}$ for all $\alpha > 0$

and only finitely many of the images of U can be disjoint from S. We thus conclude that each E^n must be a homeomorphism on U.

Now suppose there is a sequence n_j such that for each j, $E^{n_j}(U) \cap S = \phi$. By the previous lemma, $|(E^{n_j})'(z)| \geq (\pi/3)^{n_j}$ for each j and all $z \in U$. It follows that, if U contains a disk of radius $\delta > 0$, then $E^{n_j}(U)$ contains a disk of radius $\delta(\pi/3)^{n_j}$. See Exercise 2. Hence for j large enough, $E^{n_j}(U)$ must meet a line of the form $y = 2\pi$ and again we are done.

□

Lemma 4.9 *Let V be an open connected set for which infinitely many of its images are contained in the half plane $H = \{z \,|\, \text{Re } (z) > 4\}$. Then there exists $n > 0$ for which $E^n(V) \cap \mathbf{R} \neq \emptyset$.*

Proof. Let W denote the set $\{z \,|\, |\text{Im } (z)| \leq 2\pi \text{ and } |\text{Im } (E(z))| \leq 2\pi\}$. If a connected set A satisfies $A \cap W = \emptyset$, then either $A \cap S$ or $E(A) \cap S$ is empty. Consequently, by the previous lemma, only finitely many images of V in H can be disjoint from W. Hence almost all images of V are contained in W.

Now consider the boundary $|y| = \frac{\pi}{3}$ of S in H. If z lies on this boundary, then

$$|\text{Im } (E(z))| \geq e^4 \sin\left(\frac{\pi}{3}\right) > 2\pi.$$

Therefore, the boundary of S in H does not lie in W. Thus every connected set in $W \cap H$ is either contained in S or disjoint from S. Now the image of $S \cap H$ is contained in H. Since infinitely many of the images of V are contained in $W \cap H$, and since for each $z \in \mathbf{C} - \mathbf{R}$, there exists $n \geq 0$ such that $E^n(z) \notin S$ (see the proof of Proposition 4.6), it therefore follows that infinitely many of them must be disjoint from S. This contradicts Lemma 4.8.

□

We can now prove

Theorem 4.10 $J(E) = \mathbf{C}$.

Proof. By Proposition 4.6, it suffices to show that any open set in $\mathbf{C}$ contains some preimage of $\mathbf{R}$. To that end, let U be open and connected and suppose $E^n(U) \cap \mathbf{R} = \emptyset$ for each n. By Montel's Theorem, $\{E^n\}$ is a normal family on U.

Let D denote the disk of radius e^4 about 0. Note that $E(H)$ is the complement of D. Hence, by Lemma 4.9, it follows that infinitely many of the images of U meet D.

Now let F denote the limit function of some subsequence of the E^n. By the above, $F(U) \cap D \neq \phi$. Choose a point $z_0 \in F(U) \cap D$. If $z_0 \in \mathbf{R}$, then there exists $k > 0$ such that $E^k(U) \cap \mathbf{R} \neq \phi$ and we are done. Thus we assume $z_0 \notin \mathbf{R}$. As we observed in Proposition 4.6, there exists $k > 0$ for which $E^k(z_0) \notin S$. Therefore there exists $w \in U$ and another subsequence of the E^n which converges to a map F_1 which satisfies $F_1(w) \notin S$. But then there is an open neighborhood V of w and infinitely many images $E^n(V)$ which do not meet S. This contradicts Lemma 4.8 and establishes the theorem.

□

References

[A] Atela,P. Bifurcations of Dynamic Rays in Complex Polynomials of Degree Two. *Ergod. Th. & Dynam. Sys.* **12** (1991), 401-423.

[AO] Aarts, J. and Oversteegen, L. The Geometry of Julia Sets. *Trans. Amer. Math. Soc.* **338** (1993),897-918.

[B] Branner, B. The Mandelbrot Set. In *Chaos and Fractals: The Mathematics Behind the Computer Graphics.* Amer. Math. Soc. (1989) 75-106.

[BD] Bhattacharjee, R. and Devaney, R. L. Tying Hairs for Structurally Stable Exponentials. Preprint.

[Bl] Blanchard, P. Complex Analytic Dynamics on the Riemann Sphere, *B.A.M.S.* **2** (1984),85-141.

[Bo] Bodelon, C. et. al. Hairs for the Complex Exponential Family. Preprint.

[BR] Baker, I. N. and Rippon, P. Iteration of Exponential Functions, *Ann. Acad. Sci. Fenn.*, Series 1A Math. **9** (1984),49-77.

[DBDS] (Douady,A. Buff, X. Devaney, R. L. and Sentenac, P. Baby Mandelbrot Sets are Born in Cauliflowers. In *The Mandelbrot Set: Theme and Variations*, London Mathematical Society Lecture Notes, Cambridge University Press, ed. Tan Lei. **274** (2000), 19-36.

[D2] Devaney, R. L. The Structural Instability of Exp(z). *Proc. A.M.S.*, **94** (1985),545-548.

[DG] Devaney, R. L. and Goldberg, L. Uniformization of Attracting Basins for Exponential Maps. *Duke Mathematics Journal.* **55** (1987), 253-266.

[DH] Douady, A. and Hubbard, J. Étude Dynamique des Polynôme Complexes, *Publications Mathematiques d'Orsay.*

[DH1] Douady, A. and Hubbard, J. Itération des Polynômes quadratiques complexes, *C.R. Acad. Sci. Paris*, t.29, Serie I-1982, 123-126.

[DH2] Douady, A. and Hubbard, J. On the Dynamics of Polynomial-like Mappings, *Ann. Scient., Éc. Norm. Sup.* 4^e *séries*, t.18, 1985, 287.

[1] Devaney, R. L. and Jarque, X. Misiurewicz Points for Complex Exponentials *Int. J. Bifurcation and Chaos* **7** (1997), 1599-1616.

[DK] Devaney, R. L. and Krych, M. Dynamics of Exp(z), *Ergodic Theory and Dynamical Systems* **4** (1984), 35-52.

[DoG] Douady, A. and Goldberg, L. The Nonconjugacy of Certain Exponential Functions. In *Holomorphic Functions and Moduli.* MSRI Publ., Springer Verlag (1988), 1-8.

[DT] Devaney, R. L. and Tangerman, F. Dynamics of Entire Functions Near the Essential Singularity, *Ergodic Thy. Dynamical Syst.* **6** (1986), 489-503.

[EL] Eremenko, A. and Lyubich, M. Yu. Iterates of Entire Functions. *Dokl. Akad. Nauk SSSR* **279** (1984), 25-27. English translation in *Soviet Math. Dokl.* **30** (1984), 592-594.

[F] Farey, J. On a curious property of vulgar fractions. *Phil. Mag. J. London* **47** (1816), 385-386.

[Fa] Fagella, N. Limiting Dynamics for the Complex Standard Family. *Intern. J. Bifur. chaos Appl. Sci. Engrg.* **5** (1995), 673-679.

[GK] Goldberg, L. R. and Keen, L. A Finiteness Theorem For A Dynamical Class of Entire Functions, *Ergodic Theory and Dynamical Systems* **6** (1986), 183-192.

[Lav] LaVaurs,P. Une Description Combinatoire de l'involution definie par M sur les rationelles a denominateur impaire. *C. R. Acad. Sci. Paris Sér. I Math.* **303** (1986), 143-146.

[Ly] Lyubich, M. Measurable Dynamics of the Exponential, *Soviet Math. Dokl.* **35** (1987), 223-226.

[Ma] Mayer, J. An Explosion Point for the Set of Endpoints of the Julia Set of $\lambda \exp(z)$. *Erg. Thy. and Dyn. Syst.* **10** (1990), 177-184.

[McM] McMullen, C. Area and Hausdorff Dimension of Julia Sets of Entire Functions. *Trans. A.M.S.* **300** (1987), 329-342.

[Pi] Piranian, G. The Boundary of a Simply Connected Domain. *Bull. Amer. Math. Soc.* **64** (1958), 45-55.

[PM] Pomeau, Y. and Manneville, P. Intermittent Transition to Turbulence in Dissipative Dynamical Systems. *Commun. Math. Phys.* **74**, 189-197 (1980).

[S] Smale, S. Diffeomorphisms with Many Periodic Points. *Differential and Combinatorial Topology.* Princeton University Press, 1964, 63-80.

[Su] Sullivan, D., Quasiconformal Maps and Dynamical Systems I, Solutions of the Fatou-Julia Problem on Wandering Domains. *Ann. Math.* **122** (1985), 401-418.